Flux of low salinity water from Aniva Bay (Sakhalin Island) to the southern Okhotsk Sea

Sachiko Oguma*

Research Fellow of the Japan Society for the Promotion of Science,
Hokkaido National Fisheries Research Institute, Fisheries Research Agency
116 Katsurakoi, Kushiro, Hokkaido 085-0802, Japan
soguma@affrc.go.jp

Tsuneo Ono

Hokkaido National Fisheries Research Institute, Fisheries Research Agency
116 Katsurakoi, Kushiro, Hokkaido 085-0802, Japan
tono@fra.affrc.go.jp

Yutaka W. Watanabe

Faculty of Earth Environmental Science, Hokkaido University
North 10 West 5, Kita-ku, Sapporo, Hokkaido 060-0810, Japan
yywata@ees.hokudai.ac.jp

Hiromi Kasai

Hokkaido National Fisheries Research Institute, Fisheries Research Agency
116 Katsurakoi, Kushiro, Hokkaido 085-0802, Japan
kasaih@fra.affrc.go.jp

Shuichi Watanabe

Mutsu Institute for Oceanography, Japan Agency for Marine-Earth Science and Technology
690 Kita-Sekine, Mutsu, Aomori 035-0022, Japan
swata@jamstec.go.jp

Daiki Nomura

National Institute of Polar Research
10-3 Midori-cho, Tachikawa-shi, Tokyo 190-8501, Japan
nomura.daiki@nipr.ac.jp

Humio Mitsudera

Institute of Low Temperature Science, Hokkaido University
North 19 West 8, Kita-ku, Sapporo, Hokkaido 060-0819, Japan
humiom@lowtem.hokudai.ac.jp

*: corresponding author

Abstract

In this study, we examined the relationship between the low salinity water in the shelf region of the southern Okhotsk Sea which was seasonally sampled (0-200 m), and fluxes of low salinity water from Aniva Bay. To express the source of freshwater mixing in the surface layer, we applied normalized total alkalinity (NTA) and stable isotopes of seawater as chemical tracers. NTA-S diagrams indicate that NTA of low salinity water in the upper 30 m layer just off the Soya Warm Current is clearly higher than in the far offshore region in summer and autumn. Using NTA-S regression lines, we could deduce that the low salinity and high NTA water in the upper layer originates from Aniva Bay. For convenience, we defined this water as the Aniva Surface Water (ASW) with values S<32, NTA>2450 μmol kg^{-1}. Formation and transport processes of ASW are discussed using historical data. The interaction between the maximum core of high NTA water on the bottom slope of eastern Aniva Bay and an anticyclonic eddy at the mouth of Aniva Bay are concluded to control ASW formation. Upwelling of the Cold Water Belt water at the tip of Cape Krillion is considered to cause ASW outflow from Aniva Bay.

Keywords

Aniva Bay, southern Okhotsk Sea, normalized total alkalinity, stable isotopes, chemical tracers

Regional Terms

Russia, Sakhalin Island, Aniva Bay

1. Introduction

The southern Okhotsk Sea consists of a shelf region between Sakhalin Island and Hokkaido and a deep sea region in the western part of the Kuril Basin (Figure 1). In the shelf region, temperature and salinity distributions show notable seasonal variations (e.g. Itoh and Ohshima, 2000). During summer and autumn, the Soya Warm Current (SWC) flows along the coast of northeastern Hokkaido and brings warm saline subtropical water from the Japan Sea. In winter, the East Sakhalin Current (ESC) flows southward from Sakhalin Island to Hokkaido, while SWC weakens. East Sakhalin Current water (ESCW) is characterized by salinity less than 32.0 (Takizawa, 1982). Surrounding these currents, surface water with salinity less than 32.5 named Okhotsk Surface Water (OSW) distributes on the offshore side (Takizawa, 1982). OSW forms seasonal thermocline with underlying Intermediate Cold Water (ICW), which is formed by convective mixing under sea ice in winter and characterized as the temperature minimum layer (Kitani, 1973; Takizawa, 1982). Stratification between OSW and ICW formed within euphotic zone causes the formation of subsurface chlorophyll-*a* maximum during summer and autumn (Kasai et al., 2010). OSW is also considered as an optimum water mass for growth of the toxic dinoflagellate, *Alexandrium tamarense*, the causative agent of paralytic shellfish poisoning (Shimada et al., 2009). In the deep sea region, on the other hand, an anticyclonic gyre exists in the Kuril Basin, which involves mesoscale anticyclonic eddies (Wakatsuchi and Martin, 1991; Ohshima et al., 2002; Ebuchi, 2006).

OSW seems to be important for biogeochemical conditions in the southern Okhotsk Sea (e.g. Shimada et al., 2009; Kasai et al., 2010), however, formation process of OSW has not been deeply discussed, while formation processes of subsurface water masses in the Okhotsk Sea have been studied in detail (e.g. Kitani, 1973; Takizawa, 1982; Tally and Nagata, 1995; Watanabe and Wakatsuchi, 1998; Yamamoto et al., 2001). Kitani (1973) showed seasonal change of temperature and salinity of surface water in the southern Okhotsk Sea, and suggested that the salinity is lowered by the sea ice melt water and/or the inflow of river water. Takizawa (1982) suggested that OSW is freshened by sea ice melt water and/or precipitation, separating from ESCW freshened by the Amur River discharge. However, as Iida (1962) previously indicated, it is questionable that if OSW maintains a low salinity in the warm season when the sea ice has already disappeared. It is also

difficult to consider Amur River runoff as the only freshwater source of OSW especially in summer, because moving in ESC region from river mouth of Amur River would require over six months to reach to off Hokkaido (Mizuta et al., 2003).

Sugiura (1958) firstly indicated that Aniva Bay located at the southern end of Sakhalin Island (Figure 1) might lower the salinity of OSW in summer. Watanabe (1963) showed a tongue-like distribution of low salinity water from off Aniva Bay. Monthly variations of the horizontal distributions of sea surface salinity in the southern Okhotsk Sea drawn by Itoh and Ohshima (2000) also suggested that low salinity water appeared in the vicinity of the southern tip of Sakhalin Island in summer, though they classified water mass with salinity less than 32.0 as ESCW. Based on data from a recent survey in the southern Okhotsk Sea, Figure 2 shows the horizontal distribution of salinity at 10 m depth in August 1995 obtained by the Hokkaido Fisheries Experimental Station (HFES, 2004). OSW distributed just off Soya Warm Current water (SWCW) and horizontal temperature minimum water named as Cold Water Belt (CWB) (e.g. Iida, 1962; Ishizu et al., 2008). In OSW region with salinity less than 32.5, the freshest water with salinity less than 32.0 appeared from the mouth of Aniva Bay, indicating that Aniva Bay was possibly a source region of freshwater of OSW (Sugiura, 1958; Watanabe, 1963).

In this study, we examine the relationship between the low salinity water in the shelf region of the southern Okhotsk Sea, and Aniva Bay. We use oceanic data obtained seasonally at depths shallower than 200 m in the southern Okhotsk Sea. To determine the source of freshwater mixing in the surface layer, we apply total alkalinity (TA), $\delta^{13}C$ of oceanic dissolved inorganic carbon ($\delta^{13}C_{DIC}$), and $\delta^{18}O$ of seawater as chemical tracers, together with conventional water mass tracers, temperature and salinity. TA and $\delta^{18}O$ have been applied as powerful tools to distinguish freshwater sources, such as river runoff, precipitation, sea ice melt water, and brine, in the arctic and subarctic regions (e.g. Yamamoto et al., 2001, 2002; Anderson et al., 2004; Yamamoto-Kawai et al., 2005; Pavlova et al., 2008). $\delta^{13}C_{DIC}$, on the other hand, has been used to trace globally or regionally the water mass which experienced air-sea CO_2 exchange reflecting temperature at the sea surface (e.g. Broecker and Maier-Reimer, 1992; Lynch-Stieglitz et al., 1995; Itou et al., 2003). In this paper, we firstly show our observation results obtained in the southern Okhotsk Sea. We then compare these results with historical data in other areas of the Okhotsk Sea to describe the source region of low salinity water, and discuss its formation and transport processes.

2. Materials and Methods

We use data obtained in July 2004 (TKN0407, Jul 22-Aug 1, 2004), October 2004 (TKN0410, Oct 1-5, 2004) and May 2005 (TKN0505, May 11-15, 2005) along the 'N-line' off Cape Notoro during cruises of the R/V *Tankai-Maru* of the Hokkaido National Fisheries Research Institute, Fisheries Research Agency (Oguma et al., 2008; Kasai et al., 2010). Observation stations of the N-line are shown in Figure 1b. Vertical seawater sampling was operated using Niskin bottles with a rosette multi sampler at standard depth. The nutrient samples were placed in acrylic tubes and frozen on board until measurement in the laboratory. Nutrient concentrations were determined colorimetrically using Bran+Luebbe Autoanalyzer TRAACS 800 and AACS-III (Parsons et al., 1984) with nutrient reference material produced by the Kansai Environmental Engineering Center Co., Ltd. The mean difference of duplicate phosphate samples was $\sigma(PO_4)$ = 0.084 μmol/L. Samples for TA analysis were collected in 100 ml glass vials and sealed immediately. TA was determined by the method of Ono et al. (1998). Samples for $\delta^{13}C_{DIC}$ sampling were collected in 100 ml glass bottles and fixed with $HgCl_2$, while for $\delta^{18}O$ they were collected in 50 ml glass bottles. These samples were sealed on board and refrigerated in the laboratory until analysis. The measurements for $\delta^{13}C_{DIC}$ analysis were carried out following the methods detailed in Tanaka et al. (2003), while $\delta^{18}O$ was determined following Yamamoto et al. (2002). Both $\delta^{13}C_{DIC}$ and $\delta^{18}O$ were measured using a mass spectrometer (Finnigan MAT, Delta-S). The precision of replicate analyses for $\delta^{13}C_{DIC}$ (n = 17) was $\sigma(\delta^{13}C) = \pm 0.033$ ‰, and the variability of $\delta^{13}C_{DIC}$ among duplicate samples was 0.020 ± 0.015 ‰ (n = 20). The standard deviation of $\delta^{18}O$ value of differences between two standard waters (n = 119) was 0.021 ‰, and the variability of $\delta^{18}O$ among duplicate samplings was 0.026 ± 0.017 ‰ (n = 21).

We also used wintertime data obtained in the southern Okhotsk Sea by P/V *Soya* of the 1st Regional Coast Guard Headquarters, Japan, in February 2006 (Toyota, 2006; Nomura et al., 2009a, 2009b). Sampling points are shown in Figure 1b. Sea surface water samples for nutrients, TA, $\delta^{13}C_{DIC}$ and $\delta^{18}O$ were collected through cracks between sea ice floes with a bucket. Samples for nutrients and TA measurements were stored and measured following Nomura et al. (2009a), and for

$\delta^{13}C_{DIC}$ and $\delta^{18}O$ were in the same method as for the N-line samples.

To detect endmembers of the water masses flowing into the southern Okhotsk Sea, we used the oceanic data for the northern and central Okhotsk Sea obtained by R/V *Professor Khromov* of the Far Eastern Regional Hydrometeorological Research Institute, Russia, in July 1998, September 1999 and June 2000 (Wakita et al., 2003). We also used historical data of the World Ocean Database 2005 (WOD05) (Boyer et al., 2006). From WOD05, data for stations in Aniva Bay and off the southeastern coast of Sakhalin Island, where temperature, salinity and TA were observed, were extracted. They were mostly obtained in the 1960s and 1970s. Observed locations of these historical data are shown in Figure 1a.

To discuss the transport processes of sea surface water from Aniva Bay, we used zonal/meridional momentum flux (wind stress) data provided from the web site of the Japanese Ocean Flux datasets with Use of Remote Sensing Observations (J-OFURO) (http://dtsv.scc.u-tokai.ac.jp/j-ofuro/).

Before data analysis, we made an offset collection for TA data of the N-line cruises assuming that the water mass below 27.4 σ_θ has not changed over a decadal time scale (Yamamoto-Kawai et al., 2004; Watanabe et al., 2009). We compared with TA data obtained by R/V *Professor Khromov* cruises (Wakita et al., 2003) and calculated offset values for each N-line cruise based on the data sets below 27.4 σ_θ. Since TA is affected by the processes of organic matter decomposition, potential alkalinity (PA = TA + $[NO_3^-]$ - $[NH_4^+]$) is preferable in the high productive area such as the Okhotsk Sea (Pavlova et al., 2008). However, historical data obtained in Aniva Bay included few nutrient data, and then we could not calculate PA values. Although we found that nitrate considerably increased from less than 1 μmol kg^{-1} to over 20 μmol kg^{-1} at depths shallower than 200 m (Kasai et al., 2010), distribution patterns of PA and TA were not largely changed. Hereafter, we used TA in this study. To eliminate the effects of dilution by precipitation or concentration by sea ice formation, we used normalized TA, NTA, applying salinity-normalization scheme represented by Friis et al. (2003) as follows,

$$NTA = (TA - TA_0) \times 35 / S + TA_0, \qquad (1)$$

where TA_0 is a non-zero freshwater endmember and S is salinity. Here we assumed TA_0 = 589 μmol

kg^{-1} based on the climatological riverine data, which were obtained in Amur River estuary and Sakhalin Bay (Andreev and Pavlova, 2010).

We applied the isotopic ratio of stable isotopes, $\delta^{13}C$ of dissolved inorganic carbon ($\delta^{13}C_{DIC}$) and $\delta^{18}O$ of seawater, as parameters to classify the water masses in the southern Okhotsk Sea. $\delta^{13}C_{DIC}$ is affected not only by air-sea fractionation, but also by biological isotope separation during marine photosynthesis (Broecker and Maier-Reimer, 1992). The effect of air-sea CO_2 exchange on $\delta^{13}C_{DIC}$, denoted as $\delta^{13}C^*$, is calculated as follows (Broecker and Maier-Reimer, 1992; Lynch-Stieglitz et al., 1995; Itou et al., 2003; Oguma et al., 2008),

$$\delta^{13}C^* = \delta^{13}C_{DIC} - \delta^{13}C_{bio} = \delta^{13}C_{DIC} - (-1.1\ PO_4 + 2.9), \qquad (2)$$

where $\delta^{13}C_{bio}$ is biologically predicted $\delta^{13}C$ calculated from the phosphate concentration. $\delta^{13}C^*$ of offshore water has a linear negative relationship with temperature of the region where the water mass was exposed to the atmosphere (Zhang et al., 1995; Itou et al., 2003), and conserves the temperature information of the source area of the water mass after subduction (Itou et al., 2003; Oguma et al., 2008). However, $\delta^{13}C^*$ of coastal water may additionally be influenced by river water with ^{13}C-depleted calcite (e.g. Mook and Tan, 1991). $\delta^{18}O$ of seawater reflects the hydrological cycle at the sea surface. Precipitation and river water introduce ^{18}O-depleted water, and sea ice melt water leads to fluxes of $\delta^{18}O$-enriched water (e.g. Yamamoto et al., 2002).

3. Results and discussion

3.1. Water properties along the N-line

Temperature (T), salinity (S), NTA, $\delta^{13}C^*$ and $\delta^{18}O$ data shallower than 200 m obtained in July and October 2004, February 2006, and May 2005, are summarized in Figure 3, which are shown seasonally from summer to spring. The characteristic values of temperature, salinity, and isotopic ratio of stable isotopes of water masses in the southern Okhotsk Sea derived from former studies (Takizawa, 1982; Biebow et al, 2001a, 2001b; Yamamoto et al., 2001; Bauch et al., 2002;

Itou et al., 2003) are summarized in Tables 1 and 2, and they are shown in Figure 3 as the boundaries of water mass classification in the Okhotsk Sea on T-S and $\delta^{13}C^*$-$\delta^{18}O$ diagrams. In the $\delta^{13}C^*$-$\delta^{18}O$ diagrams, if freshwater is supplied from precipitation, only $\delta^{18}O$ is depleted. However, if river water is mixed, then both $\delta^{13}C^*$ and $\delta^{18}O$ are depleted. The shift in directions of plots caused by freshwater mixing is schematically shown as arrows in the $\delta^{13}C^*$-$\delta^{18}O$ diagrams.

To eliminate the effect of sea ice formation on the salinity data obtained in February 2006, we back-calculate the original salinity, S_{org}, from the $\delta^{18}O$ value using the linear relationship (S_{org} = ($\delta^{18}O$ + 13.561) / 0.3915) obtained for the western subarctic Pacific region (Yamamoto et al., 2001). Figure 4 shows that the most of data obtained at Sts. N02-N04 show close agreement with the S-$\delta^{18}O$ linear relationship. Coastal water obtained at St. N01 deviated to $\delta^{18}O$-enriched side from the linear relationship due to SWCW (Oguma et al., 2008). $\delta^{18}O$-depletion of subsurface water (26.8-27.0 σ_θ) with salinity over 33.6 at St. N02, which are emphasized by dotted circle in Figure 4, may be affected by dense shelf water from the northern Okhotsk Sea (Yamamoto et al., 2002). It is suggested that salinity values obtained at Sts. 5 and 13 are lowered by sea ice melting water, and those obtained at Sts. 6, 10, and 19 are enhanced by brine formation. Here we estimate S_{org} for these stations related with sea ice, and then we recalculate original NTA, NTA_{org}. S_{org} and NTA_{org} values are shown in Figure 3c.

Following the water mass classifications on T-S diagrams by Takizawa (1982), surface water shallower than 26.0 σ_θ were roughly divided into SWCW at the most coastal St. N01 and OSW at offshore Sts. N02-N04 in summer and autumn (Figure 3a and 3b). Under OSW, ICW distributes around 26.5 σ_θ. Since SWC is weakened and ESC is forced in winter (Watanabe, 1963; Itoh and Ohshima, 2000), low salinity water classified as OSW occurs instead of SWCW at coastal Sts. 5, 6, 17, and 19 (Figure 3c). Forerunner of SWCW (f-SWCW) (Takizawa, 1982) occurs only at St.1 near the Soya Strait. In spring, subsurface layer water at St. N01 seems to be mixed with f-SWCW but mostly classified as ICW, as well as offshore Sts. N02-N04 (Figure 3d).

NTA-S diagrams suggest that NTA of water in the upper 30 m depth at St. N02 is clearly high in summer and autumn, while salinity is the same as Sts. N03 and N04. Such high NTA water is not found in spring. Here we estimate NTA-S regression lines for water shallower than 200 m depth at St. N02 in summer and autumn,

$$NTA = (-88.04 \pm 4.23)\ S + (5287.30 \pm 139.33), \quad (n = 14, r^2 = 0.973) \qquad (3)$$

and at offshore Sts. N03 and N04,

$$NTA = (-13.64 \pm 2.43)\ S + (2816.09 \pm 80.08). \quad (n = 28, r^2 = 0.547) \qquad (4)$$

NTA_{org} values in winter, which are recalculated using S_{org}, seem to be in the middle of (3) and (4). NTA-S plots of subtropical SWCW at St. N01 in summer and autumn shift lower from line (4) estimated for subarctic water. NTA-S regression lines (3) and (4) suggest a possibility of detailed classification of OSW. To examine this classification method for other regions of the Okhotsk Sea, we show the results of oceanic data in other regions of the Okhotsk Sea and historical data in following section.

$\delta^{13}C^*$-$\delta^{18}O$ diagram in summer (Figure 3a) indicates that surface water in the upper 30 m at Sts. N02-N04 is relatively $\delta^{18}O$-depleted from the range of the central Okhotsk water (c-OW). It is notable that $\delta^{13}C^*$ in the upper 30 m depths at St. N02 is not depleted. This result suggests that the surface water at St. N02 is not affected by river water discharge. As Takizawa (1982) suggested, salinity of OSW would be lowered due to precipitation in summer. $\delta^{13}C^*$-depletion and slight $\delta^{18}O$-enrichment under the temperature minimum layer within ICW would be occurred by intrusion of the f-SWCW (Takizawa, 1982; Watanabe and Wakatsuchi, 1998; Oguma et al., 2008). In autumn (Figure 3b), $\delta^{13}C^*$ in the upper 30 m depth at Sts. N02-N04 is depleted, while $\delta^{18}O$ is more depleted at St. N02 but is less depleted at Sts. N03 and N04 from summer. This result may be caused by mixing with river waters from different sources. Since ESCW which is affected by the Amur River discharge still distributes far north from Hokkaido in October (Mizuta et al., 2003), the surface water at offshore Sts. N03 and N04 can mix with ESCW. However, it is difficult at relatively near shore St. N02. In winter (Figure 3c), sea surface water at most stations off northeastern Hokkaido, except for St. 1 near the Soya Strait and offshore-most St. 13, indicate an influence of ESCW. In spring (Figure 3d), $\delta^{13}C^*$ and $\delta^{18}O$ values of Sts. N02-N04 are mostly in c-OW area, but those of St. N01 shift to values approximating the SWCW area suggesting the occurrence of f-SWCW.

3.2. Source region of low salinity and high NTA water

Figure 5 shows NTA-S diagram of data at depth shallower than 200 m in the northern and central Okhotsk Sea obtained by R/V *Professor Khromov,* and of data for Aniva Bay and off the southeastern coast of Sakhalin Island contained in WOD05. The data concentrating around NTA = 2540-2580 μmol kg^{-1}, which were obtained from May 1971 to August 1971, are excluded from the data analysis. Comparing with regression line (3) estimated for water obtained at St. N02 and line (4) for water at Sts. N03 and N04, line (3) fits to NTA-S plots of water in Aniva Bay, and line (4) leans to plots of low salinity and high NTA water in the northern Okhotsk Sea affected by the Amur River discharge. NTA-S plots of water off the southeastern coast of Sakhalin Island also distribute along line (3). However, ESC which flows directly southward from eastern Sakhalin to northeastern Hokkaido in winter starts to strengthen in summer (Mizuta et al., 2003). Consequently, we can suggest that the low salinity and high NTA water in the upper 30 m depth layer obtained at St. N02 originates from Aniva Bay. Hereafter, we call this water as the Aniva Surface Water (ASW). For convenience, the range of salinity and NTA of ASW are defined as S<32.0 and NTA>2450 μmol kg^{-1}, respectively. Although the cause of the high NTA in Aniva Bay is not clear, NTA-S diagram can be a convenient tool for detailed water mass classification of OSW, even in the case when salinity values in surface layer show only minimal differences as shown in Figure 3a.

3.3. Formation process of ASW

Using historical data of WOD05, temperature, salinity and NTA distributions in Aniva Bay in August 1970 and October 1968 are shown in Figure 6 and Figure 7, respectively. In both cases, a warm and low salinity eddy is formed at the center of the mouth of Aniva Bay. Drifter trajectories or satellite altimeter also suggested an anticyclonic flow in this area (Ohshima et al., 2002; Ebuchi, 2006). Hereafter we call this anticyclonic eddy as Aniva Bay Eddy (ABE).

In August 1970 (Figure 6), meridional distributions indicate that cold saline water (S>34) appears on the shelf of Aniva Bay. Following the water mass classifications of Takizawa (1982), this cold saline water is much colder than SWCW or f-SWCW. However, NTA value is lower than 2360 μmol kg^{-1} the same as SWCW obtained at St. N01 (Figure 3a or 3b). It is suggested that

cooled SWCW may intrude eastward from the Soya Strait and then cause the anticyclonic flow. Longitudinal sections show that low salinity water less than 32 at the sea surface shifts to the eastern side of ABE, and the maximum core of high NTA water over 2500 μmol kg^{-1} distributes on the bottom slope of eastern Aniva Bay. It is plausible that SWCW intruding along the coastline may cause perturbations on the shelf south of Cape Aniva. Convergence of the surface water of ABE causes an upwelling of high NTA water to be freshened at the sea surface by precipitation and/or river water.

In October 1968 (Figure 7), on the other hand, horizontal temperature minimum region, which is considered as CWB, appears between SWC and ABE. Instead of SWCW, a cold water which can be classified as ICW (Takizawa, 1982) distributes on the shelf along the coastline of Aniva Bay. Horizontal distribution suggests that CWB prevents intrusion of SWCW into Aniva Bay. ICW may be entrained by weak northeastward baroclinic flow in lower layer off SWC (Ishizu et al., 2008). It is notable that high NTA water over 2450 μmol kg^{-1} mostly accounts for the water mass in Aniva Bay. In this case, ABE seems to contact directly with the shelf and to involve high NTA water on the shelf by upwelling processes as well as in August 1970. As a result, whole ABE contains very high NTA water. In this case, it is also notable that ASW spreads out southeastward from the ABE region.

3.4. Transport process of ASW

Comparing with Figures 6 and 7, CWB seems to be related to the distribution of ASW. CWB is considered that its water mass is formed by an upwelling around Cape Krillion, the western side of Aniva Bay, and is maintained by the convergence of bottom Ekman transport off the SWC region (Ishizu et al., 2006). We hypothesize as follows; ASW is entrained southeastward when CWB appears at the tip of Cape Krillion as shown in Figure 7, whereas ASW is trapped in the ABE region when SWCW intrudes into Aniva Bay and upwelling of CWB water does not occur as shown in Figure 6. In 2004, CWB was observed off SWC (Shimada et al., 2009). Satellite imagery of sea surface temperature (e.g. MODIS Near Real Time Data in JAXA/EORC website, http://kuroshio.eorc.jaxa.jp/ADEOS/mod_nrt_new/index.html, not shown here) also shows that CWB appeared in May and disappeared in November. Namely, ASW obtained in July and October

2004 is entrained by CWB water from the ABE region.

After ASW entrained by CWB water flows out from the ABE region, it is expected to advect southeastward as shown in Figure 2. As ASW distributes in the surface layer shallower than 30 m, Ekman transport by wind stress at the sea surface may be effective. Ekman transport occurs perpendicular to the right of the wind in the Northern Hemisphere, therefore, northeastward wind stress is preferable. Figure 8 shows the daily mean momentum flux distribution in June 22-July 21 and September 1-30, 2004, provided by J-OFURO. Each period is one month before the observations in July and October 2004. In September 2004, wind stress over the southern Okhotsk Sea frequently directs northeastward. Such conditions can cause southeastward flow at the sea surface. On the other hand, in June-July, wind stress direction does not bias to constant direction. This result suggests that Ekman transport is not the main process to maintain the southeastward advection of ASW off SWC.

Figure 3a and 3b show that the density of ASW at St. N02 is less than that of OSW at offshore Sts. N03-N04. It is surmised that ASW seems to flow geostrophically southeastward adjacent to heavier OSW after the entrainment by upwelling of CWB water. ADCP data of Ishizu et al. (2008) showed a very weak southeastward flow off SWC which corresponds to horizontal salinity minimum water supposed ASW. To discuss the transport process of ASW sufficiently, further observations and theoretical explanation of the advection system of ASW are necessary.

4. Conclusions

In this study, we classified the low salinity waters in the southern Okhotsk Sea using NTA, $\delta^{13}C^*$ and $\delta^{18}O$ as chemical tracers. NTA-S diagram could classify the low salinity and high NTA water just off SWC from other low salinity water masses in the OSW region. Comparing with historical data in other areas of the Okhotsk Sea, NTA-S regression lines indicated that high NTA water originated from Aniva Bay. We defined the water with values $S<32$, NTA>2450 μmol kg^{-1} as ASW. Using historical data of WOD05, we described the ASW formation process controlled by the anticyclonic ABE, which cause upwelling of high NTA water from the shelf south of Cape Aniva. We found that the outflow of ASW from Aniva Bay was related to the upwelling of CWB water.

Further discussion of the advection system of ASW off SWC still remain, however, we could show that Aniva Bay is a source of the low salinity water in the shelf region of the southern Okhotsk Sea.

Acknowledgements

We greatly thank the captains, crews and all the scientists for their help during cruises of R/V *Tankai Maru* of the Hokkaido National Fisheries Research Institute, Japan, and R/V *Professor Khromov* of the Far Eastern Regional Hydrometeorological Research Institute, Russia. We are grateful to Dr. Takenobu Toyota and the Hydrographic and Oceanographic Department of 1st Regional Coast Guard Headquarters for use of SIRAS-06 dataset obtained by P/V *Soya*. We would like to thank Dr. Mayumi Sawada for providing oceanographic data of the Hokkaido Central Fisheries Experiment Station, and Dr. Masahide Wakita for providing data of R/V *Professor Khromov* cruises. We express our hearty thanks to Prof. Hisayuki Yoshikawa-Inoue, Prof. Shinichiro Noriki, Ms. Tomomi Takamura, Ms. Satomi Komukai, Dr. Takayuki Tanaka, Dr. Yoshiyuki Nakano, Dr. Michiyo Yamamoto-Kawai, Dr. Naoyuki Kurita, Mr. Kazuhiro Hamahara, Prof. Kunio Kutsuwada, and Dr. Chris Norman for their useful advice and technical support. This study was partly supported by the Grant-in-Aid for Scientific Research and the Research Fellowship of the Japan Society for the Promotion of Science for Young Scientists.

References

Anderson, L.G., Jutterström, S., Kaltin, S., Jones, E.P., Björk, G., 2004. Variability in river runoff distribution in the Eurasian Basin of the Arctic Ocean. Journal of Geophysical Research 109, doi:10.1029/2003JC001773.

Andreev, A.G., Pavlova, G.Y., 2010. Marginal sea. In: Liu, K.-K., Atkinson L., Quiñones, R., Talaue-McManus, L. (Eds.), Carbon and Nutrient Fluxes in Continental Margins. Springer, New York, NY, pp. 395-406.

Bauch, D., Erlenkeuser, H., Winckler, G., Pavlova, G., Thiede, J., 2002. Carbon isotopes and habitat of polar planktic foraminifera in the Okhotsk Sea: the 'carbonate ion effect' under natural conditions. Marine Micropaleontology 45, 83-99.

Biebow, N., Hütten, E., Wallmann, K., 2001a. Water chemistry at station LV28-14-1. PANGAEA, doi:10.1594/PANGAEA.64753.

Biebow, N., Hütten, E., Wallmann K., 2001b. Water chemistry at station LV28-43-1. PANGAEA, doi:10.1594/PANGAEA.64761.

Boyer, T.P., Antonov, J.I., Garcia, H.E., Johnson, D.R., Locarnini, R.A., Mishonov, A.V., Pitcher, M.T., Baranova, O.K., Smolyar, I.V., 2006. World Ocean Database 2005, Levitus, S. (Ed.), NOAA Atlas NESDIS 60, U.S. Government Printing Office, Washington, D.C., 190 pp., DVDs.

Broecker, W.S., Maier-Reimer, E., 1992. The influence of the air and sea exchange on the carbon isotope distribution in the sea. Global Biogeochemical Cycles 6, 315-320.

Ebuchi, N., 2006. Seasonal and interannual variations in the East Sakhalin Current revealed by TOPEX/POSEIDON altimeter data. Journal of Oceanography 62, 171-183.

Friis, K., Körtzinger, A., Wallece, D.W.R., 2003. The salinity normalization of marine inorganic carbon chemistry data. Geophysical Research Letters 30, doi:10.1029/2002GL015898.

Hokkaido Fisheries Experimental Station (HFES), 2004. Data Record of Oceanographic Observations, No.11, April 1995 - March 1996, 216 pp.

Iida, H., 1962. On the water masses in the coastal region of the south-weatern Okhotsk Sea. Journal of the Oceanographical Society of Japan, 20th anniversary volume 272-278.

Ishizu, M., Kitade, Y., Matsuyama, M., 2006. Formation mechanism of the Cold-Water Belt formed off the Soya Warm Current. Journal of Oceanography 62, 457-471.

Ishizu, M., Kitade, Y., Matsuyama, M., 2008. Characteristics of the cold-water belt formed off Soya Warm Current. Journal of Geophysical Research 113, doi:10.1029/2008JC004786.

Itoh, M., Ohshima, K.I., 2000. Seasonal variations of water masses and sea level in the southwestern part of the Okhotsk Sea. Journal of Oceanography 56, 643-654.

Itou, M., Ono, T., Noriki, S., 2003. Provenance of intermediate waters in the western North Pacific deduced from thermodynamic imprint on $\delta^{13}C$ of DIC. Journal of Geophysical Research 108, 3347, doi:10.1029/2002JC001746.

Kasai, H., Nakano, Y., Ono, T., Tsuda, A., 2010. Seasonal change of oceanographic conditions and chlorophyll a vertical distribution in the southwestern Okhotsk Sea during the non-iced season. Journal of Oceanography 66, 13-26.

Kitani, K., 1973. An oceanographic study of the Okhotsk Sea - particularly in regard to cold waters. Bulletin of Far Seas Fisheries Research Laboratory 9, 45-77.

Lynch-Stieglitz, J., Stocker, T.F., Broecker, W.S., Fairbanks, R.G., 1995: The influence of air-sea exchange on the isotopic composition of oceanic carbon: Observations and modeling. Global Biogeochemical Cycles 9, 653-665.

Mizuta G., Fukamachi, Y., Ohshima, K.I., Wakatsuchi, M., 2003. Structure and seasonal variability of the East Sakhalin Current. Journal of Physical Oceanography 33, 2430-2445.

Mook, W.G., Tan, F.C., 1991. Stable carbon isotopes in rivers and estuaries. In: Degens, E.T., Kempe, S., Richey, J.E. (Eds.), SCOPE 42, Biogeochemistry of Major World Rivers, ICSU SCOPE Series online library (http://www.icsu-scope.org).

Nomura, D., Takatsuka, T., Ishikawa, M., Kawamura, T., Shirasawa, K.,Yoshikawa-Inoue, H., 2009a. Transport of chemical components in sea ice and under-ice water during melting in the seasonally ice-covered Saroma-ko Lagoon, Hokkaido, Japan. Estuarine, Coastal and Shelf Science 81, 201–209.

Nomura, D., Nishioka, J., Granskog, M.A., Krell, A., Matoba, S., Toyota, T., Hattori, H., Shirasawa,

K., 2009b. Nutrient distributions associated with snow and sediment-laden layers in sea ice of the southern Sea of Okhotsk. Marine Chemistry, doi:10.1016/j.marchem.2009.11.005.

Oguma, S., Ono, T., Kusaka, A., Kasai, H., Kawasaki, Y., Azumaya, T., 2008. Isotopic tracers for water masses in the coastal region of eastern Hokkaido. Journal of Oceanography 64, 525-539.

Ohshima, K.I., Wakatsuchi, M., Fukamachi, Y., Mizuta, G., 2002. Near-surface circulation and tidal currents of the Okhotsk Sea observed with satellite-tracked drifters. Journal of Geophysical Research 107, doi:10.1029/2001JC001005.

Ono, T., Watanabe, S., Okuda, K., Fukasawa, M., 1998. Distribution of total carbonate and related properties in the North Pacific along 30^{o}N. Journal of Geophysical Research 103, 30873-30883.

Parsons, T.R., Maita, Y., Lalli, C.M., 1984. A manual of Chemical and Biological Methods for Seawater Analysis. Pergamon Press, Oxford, 173 pp.

Pavlova, G.Y., Tishchenko, P.Y., Nedashkovskii, A.P., 2008. Distribution of alkalinity and dissolved calcium in the Sea of Okhotsk. Oceanology 48, 23-32.

Shimada, H., Sawada, M., Kuribayashi, T., Nakata, A., Miyazono, A., Asami, H., 2009. Spatial distribution of the toxic dinoflagellate, *Alexandrium tamarense*, in summer in the Okhotsk Sea off Hokkaido, Japan. Proceedings of the Fourth Workshop on the Okhotsk Sea and Adjacent Areas. PICES Scientific Report No. 36, Canada, 227-232.

Sugiura, J., 1958. On the sea condition in the Okhotsk Sea. Bulletin of the Hakodate Marine Observatory 5, 549-553 (in Japanese with English abstract).

Takizawa, T., 1982. Characteristics of the Soya Warm Current in the Okhotsk Sea. Journal of the Oceanographical Society of Japan 38, 281-292.

Talley, L.D., Nagata, Y. (Eds.), 1995. The Okhotsk Sea and Oyashio Region. PICES Scientific Report No.2, North Pacific Marine Science Organization (PICES), B.C., Canada, 227 pp.

Tanaka, T., Watanabe, Y.W., Watanabe, S., Noriki, S., Tsurushima, N., Nojiri, Y., 2003. Oceanic Suess effect of δ^{13}C in subpolar region: The North Pacific. Geophysical Research Letters 30, doi:10.1029/2003GL018503.

Toyota, T. (Ed.), 2006. Sea Ice Research Activities by P/V *Soya* in 2006 (SIRAS-06), Cruise Report

Vol. 3, Institute of Low Temperature Science, Hokkaido University, 72 pp.

Wakatsuchi, M., Martin, S., 1991. Water circulation in the Kuril Basin of the Okhotsk Sea and its relation to eddy formation. Journal of the Oceanographical Society of Japan 47, 152-168.

Wakita, M., Watanabe, Y.W., Watanabe, S., Noriki., S., Wakatsuchi, M., 2003. Oceanic uptake rate of anthropogenic CO_2 in a subpolar marginal sea: the Sea of Okhotsk. Geophysical Research Letters 30, doi:10.1029/2003GL018057.

Watanabe, K., 1963. On the reinforcement of the East Sakhalin Current preceding to the Sea Ice Season off the coast of Hokkaido. The Oceanographical Magazine 14, 117-130.

Watanabe, T., Wakatsuchi, M., 1998. Formation of 26.8-26.9 σ_θ water in the Kuril Basin of the Sea of Okhotsk as a possible origin of North Pacific Intermediate Water. Journal of Geophysical Research 103, 2849-2865.

Watanabe, Y.W., Nishioka, J., Shigemitsu, M., Mimura, A., Nakatsuka, T., 2009. Influence of riverine alkalinity on carbonate species in the Okhotsk Sea. Geophysical Research Letters 36, doi:10.1029/2009GL038520.

Yamamoto, M., Tanaka, N., Tsunogai, S., 2001. Okhotsk Sea intermediate water formation deduced from oxygen isotope systematics. Journal of Geophysical Research 106, C12, 31075-31084.

Yamamoto, M., Watanabe, S., Tsunogai, S., Wakatsuchi, M., 2002. Effects of sea ice formation and diapycnal mixing on the Okhotsk Sea intermediate water clarified with oxygen isotopes. Deep-Sea Research Part I 49, 1165-1174.

Yamamoto-Kawai, M., Watanabe, S., Tsunogai, S., Wakatsuchi, M., 2004. Chlorofluorocarbons in the Sea of Okhotsk: Ventilation of the intermediate water. Journal of Geophysical Research 109, doi:10.1029/2003JC001919.

Yamamoto-Kawai, M., Tanaka, N., Pivovarov, S., 2005. Freshwater and brine behaviors in the Arctic Ocean deduced from historical data of $\delta^{18}O$ and alkalinity (1929-2002 A.D.). Journal of Geophysical Research 110, doi:10.1029/2004JC002793.

Zhang, J., Quay, P.D., Wilbur, D.O., 1995. Carbon isotope fractionation during gas-water exchange and dissolution of CO_2. Geochimica et Cosmochimica Acta 59, 107-114.

Captions

Table 1: Characteristic values of temperature and salinity of water masses in the southern Okhotsk Sea (after Takizawa, 1982).

Table 2: Characteristic values of $\delta^{13}C^*$ and $\delta^{18}O$ of water masses in the southern Okhotsk Sea (Biebow et al, 2001a, 2001b; Yamamoto et al., 2001; Bauch et al., 2002; Itou et al., 2003).

Figure 1: Map of stations and bottom topography of the Okhotsk Sea. (a) Stations surveyed by the R/V *Professor Khromov* are shown by black circles, and stations in Aniva Bay and eastern side of Cape Aniva are shown by white triangles and pluses, respectively. Rectangle indicates the area shown in Figure 1b. (b) Stations surveyed by the R/V *Tankai-Maru* and P/V *Soya* are shown by black circles and white boxes, respectively. Numerals indicate station numbers. Schematics of the Soya Warm Current (SWC) and the East Sakhalin Current (ESC) are also shown.

Figure 2: Horizontal distribution of (upper) temperature and (lower) salinity at 10 m depth obtained by the Hokkaido Fisheries Experimental Station in August 1995. The area with salinity less than 32 is shaded.

Figure 3: Diagrams of temperature-salinity (T-S), normalized total alkalinity-salinity (NTA-S), and $\delta^{13}C^*$-$\delta^{18}O$ for water shallower than 200 m depth obtained during the N-line cruise in (a) July 2004, (b) October 2004, (c) February 2006, and (d) May 2005, respectively. In Figure 3a, 3b and 3d, crosses indicate data obtained at St. N01, white (black) triangles for data in 10-30 m layer (and 50-200 m layer) at St. N02, and white (black) circles for data in 10-30 m layer (and 50-200 m layer) at Sts. N03 and N04. In Figure 3c, white boxes show observed data and black boxes show recalculated data using 'original salinity', S_{org}, which is back-calculated using S-$\delta^{18}O$ linear relationship shown in Figure 4, and numerals indicate station numbers of SIRAS-06 cruise. Solid (dotted) line is NTA-S regression line calculated as equation 3 (4) for water at shallower than 200 m depth obtained at St. N02 (Sts. N03 and N04). Gray thick lines in diagrams of T-S and $\delta^{13}C^*$-$\delta^{18}O$ show water mass classifications referencing former studies, summarized in Tables 1 and 2. The shift in directions of plots caused by mixing with precipitation (PC) or river water (RW) is schematically shown as arrows in the $\delta^{13}C^*$-$\delta^{18}O$ diagrams.

Figure 4: S-$\delta^{18}O$ plot of water in the southern Okhotsk Sea obtained during N-line cruises and SIRAS-06. Symbols and numerals are the same as Figure 3. Solid line expresses S-$\delta^{18}O$ linear relationship for the western subarctic Pacific region (Yamamoto et al., 2001). Dotted circle indicates water which would be affected by dense shelf water.

Figure 5: NTA-S diagram of historical data of water shallower than 200 m depth in the Okhotsk Sea. Data obtained in the northern and central Okhotsk Sea by R/V *Professor Khromov* are shown by black circles, and WOD05 data obtained in Aniva Bay and the eastern side of Cape Aniva are shown by white triangles and pluses, respectively. Solid and dotted lines are NTA-S regression lines calculated as equations 3 and 4. Gray symbols indicate data obtained from May 1971 to August 1971, which are excluded from the data analysis.

Figure 6: Vertical distributions of (left) longitudinal section at 46-46.03^{o}N, (center) meridional section at 142.9-143.1^{o}E, and (right) 30 m depth horizontal distributions of (top) temperature, (middle) salinity, and (bottom) NTA in Aniva Bay obtained in August 1970. Contour interval of temperature, salinity, and NTA is 1^{o}C, 0.2, 20 μmol kg^{-1}, respectively. Dotted lines in NTA distributions are contours for 2450 μmol kg^{-1}. The area with salinity less than 32 or NTA over 2450 μmol kg^{-1} is shaded in vertical distributions.

Figure 7: As Figure 6, except in October 1968.

Figure 8: Daily mean momentum flux fields provided by J-OFURO in (upper) June 22-July 21, 2004 and (lower) September 1-30, 2004. All vectors obtained in each period are superimposed on each grid.

Water mass	Temperature (^{o}C)	Salinity
Okhotsk Surface Water (OSW)	< 18	< 32.5
East Sakhalin Current Water (ESCW)	< 7	< 32.0
Soya Warm Current Water (SWCW)	7 ~ 20	33.6 ~ 34.3
Forerunner of Soya Warm Current Water (f-SWCW)	2 ~ 6	33.8 ~ 34.2
Intermediate Cold Water (ICW)	-1.8 ~ +2	32.8 ~ 33.4

Table 1 Oguma et al.

Water mass	$\delta^{13}C^{*}$ (‰)	$\delta^{18}O$ (‰)
Soya Warm Current Water (SWCW)	-2.13 ~ -1.58	-0.09 ~ -0.03
East Sakhalin Current Water (ESCW)	-1.22$^{(\#)}$	-5.77 ~ -0.89
Central Okhotsk Sea Water (c-OW)	-0.63 ~ +0.09	-0.83 ~ -0.58

#: data obtained at only one layer

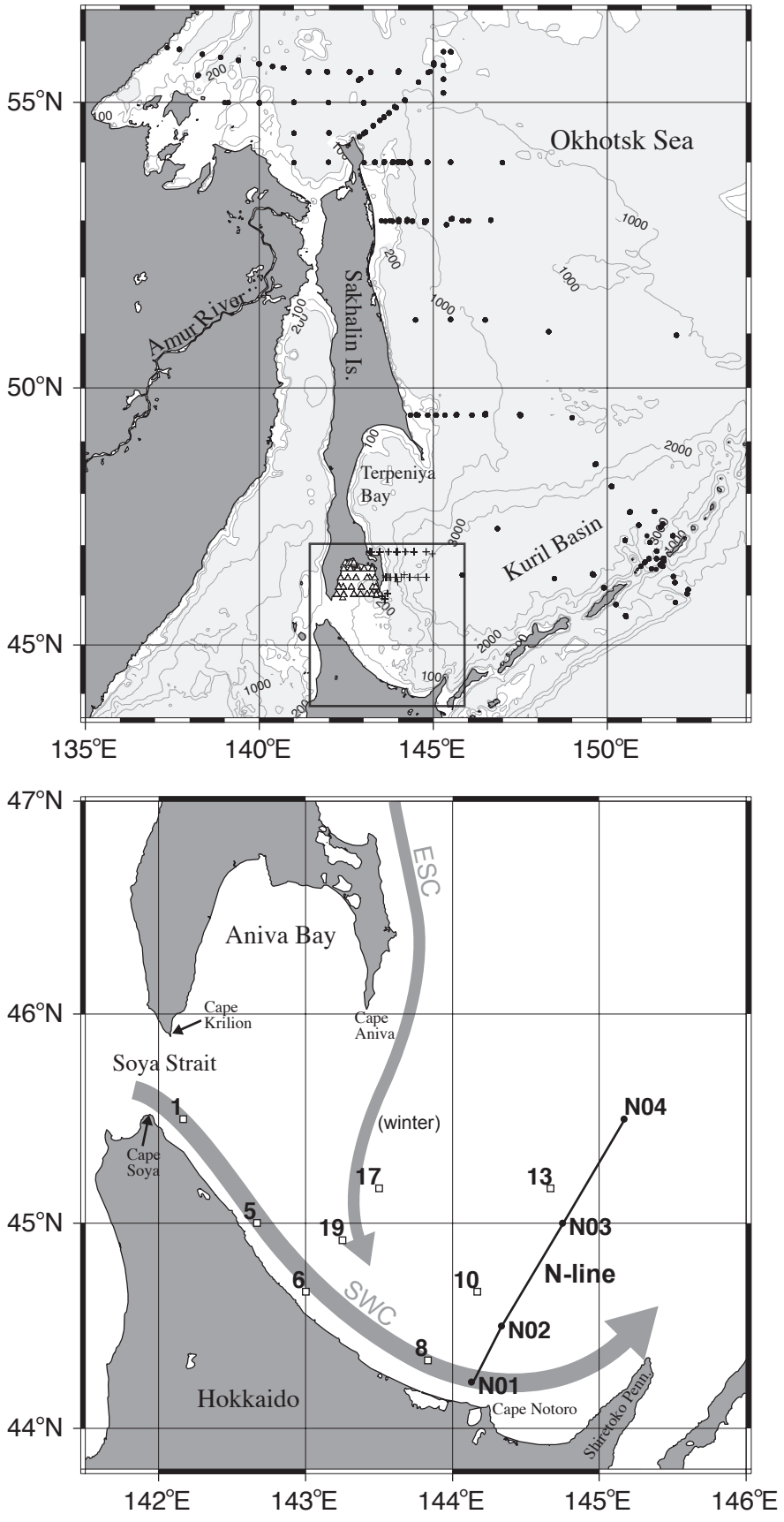

Figure 1 Oguma et al.

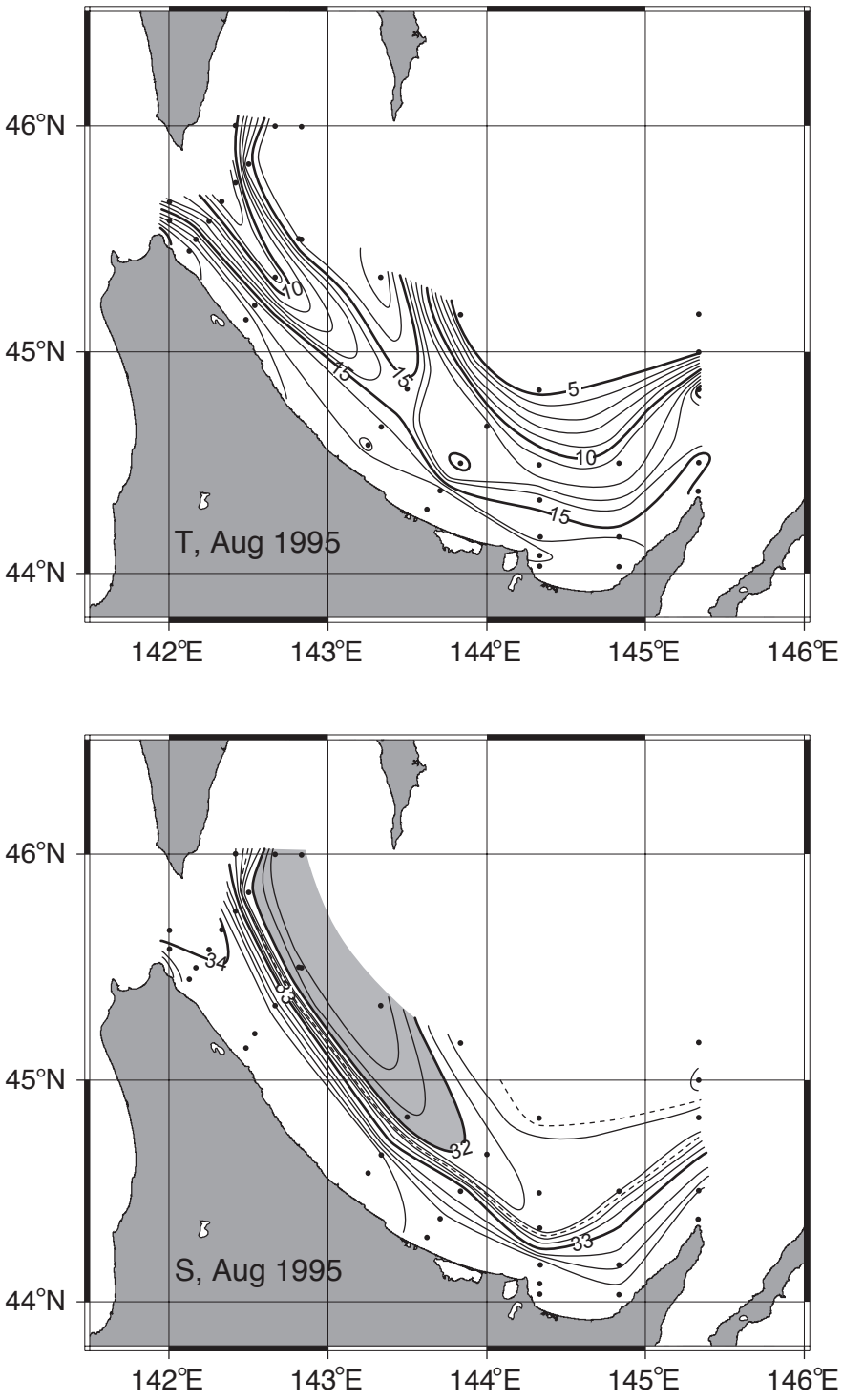

Figure 2 Oguma et al.

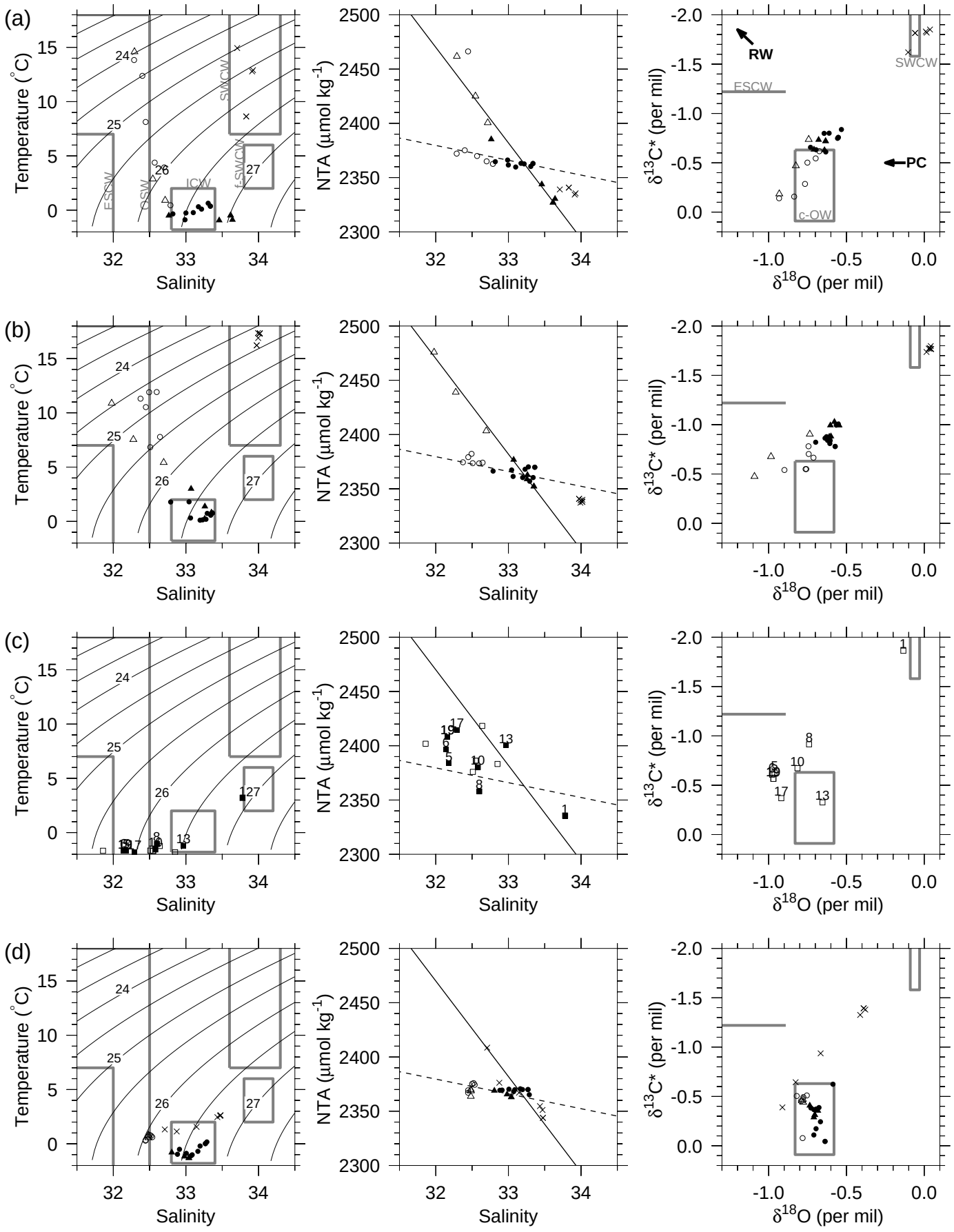

Figure 3

Oguma et al.

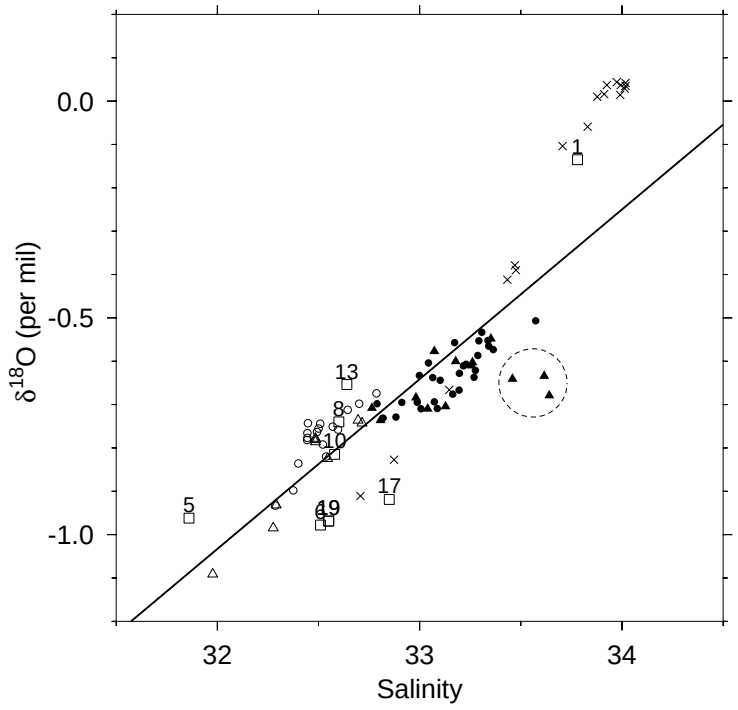

Figure 4 Oguma et al.

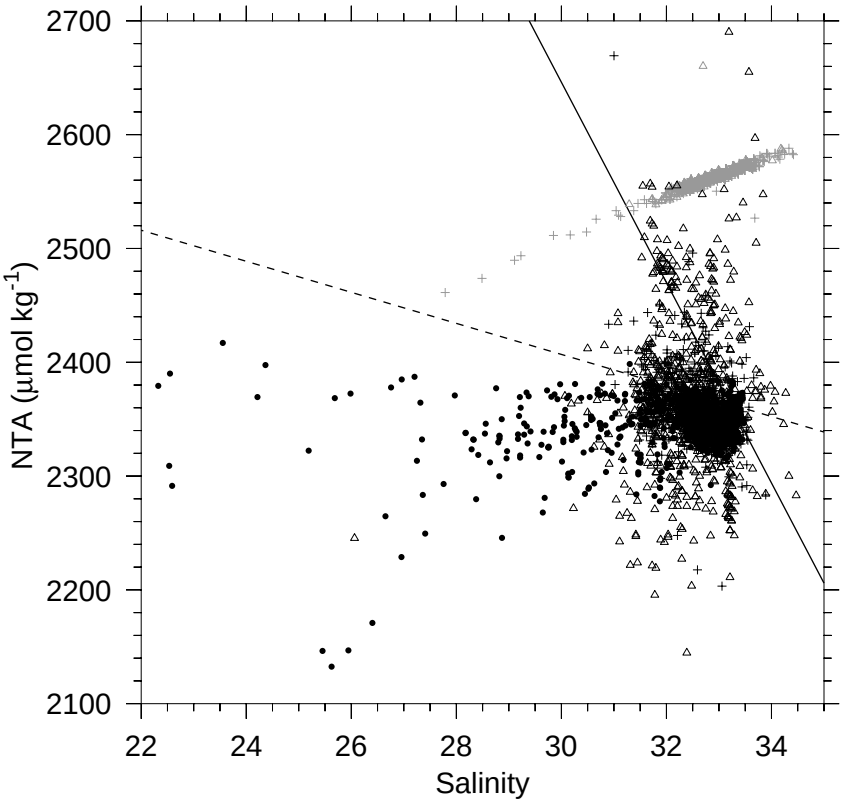

Figure 5 Oguma et al.

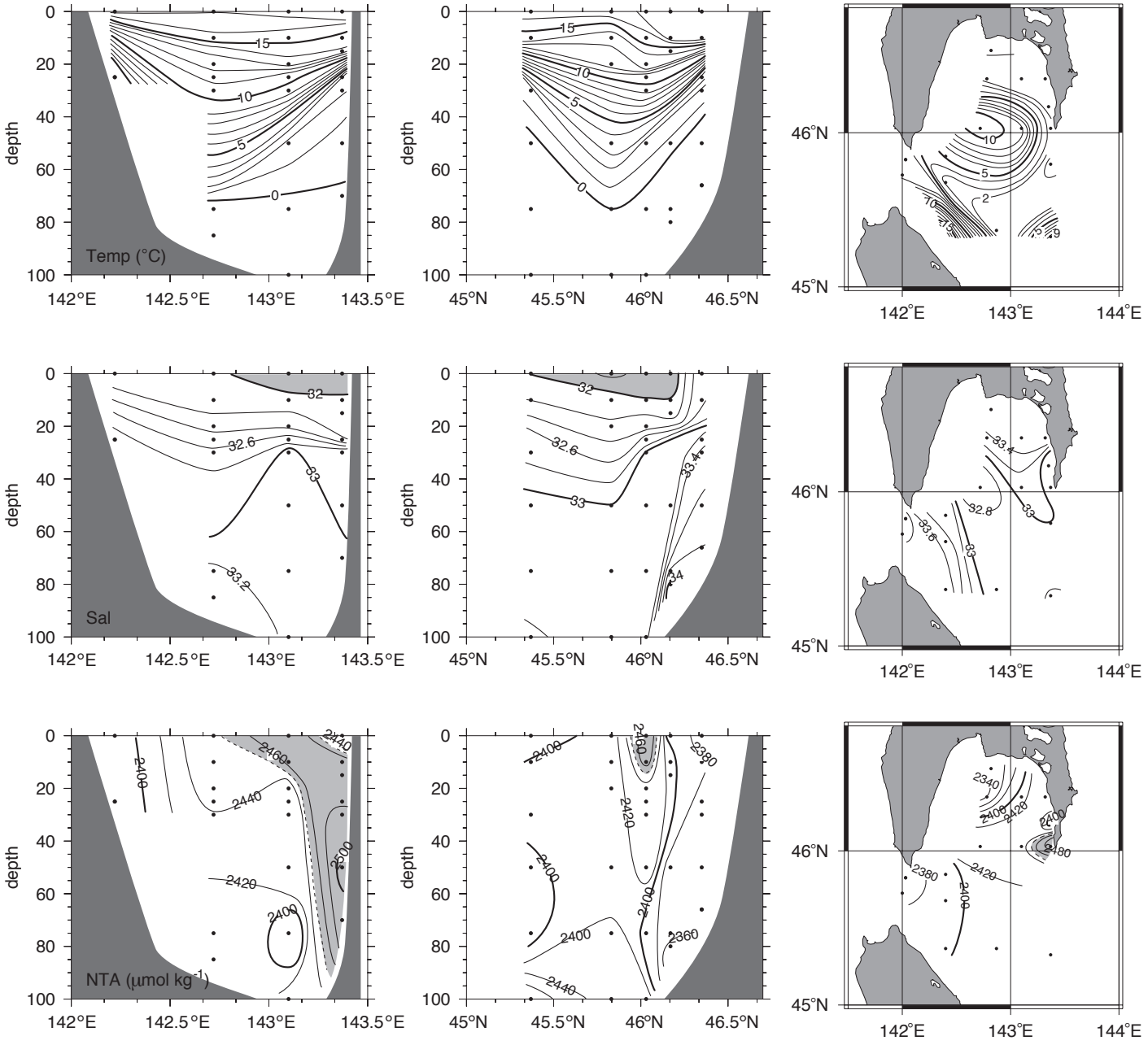

Figure 6 Oguma et al.

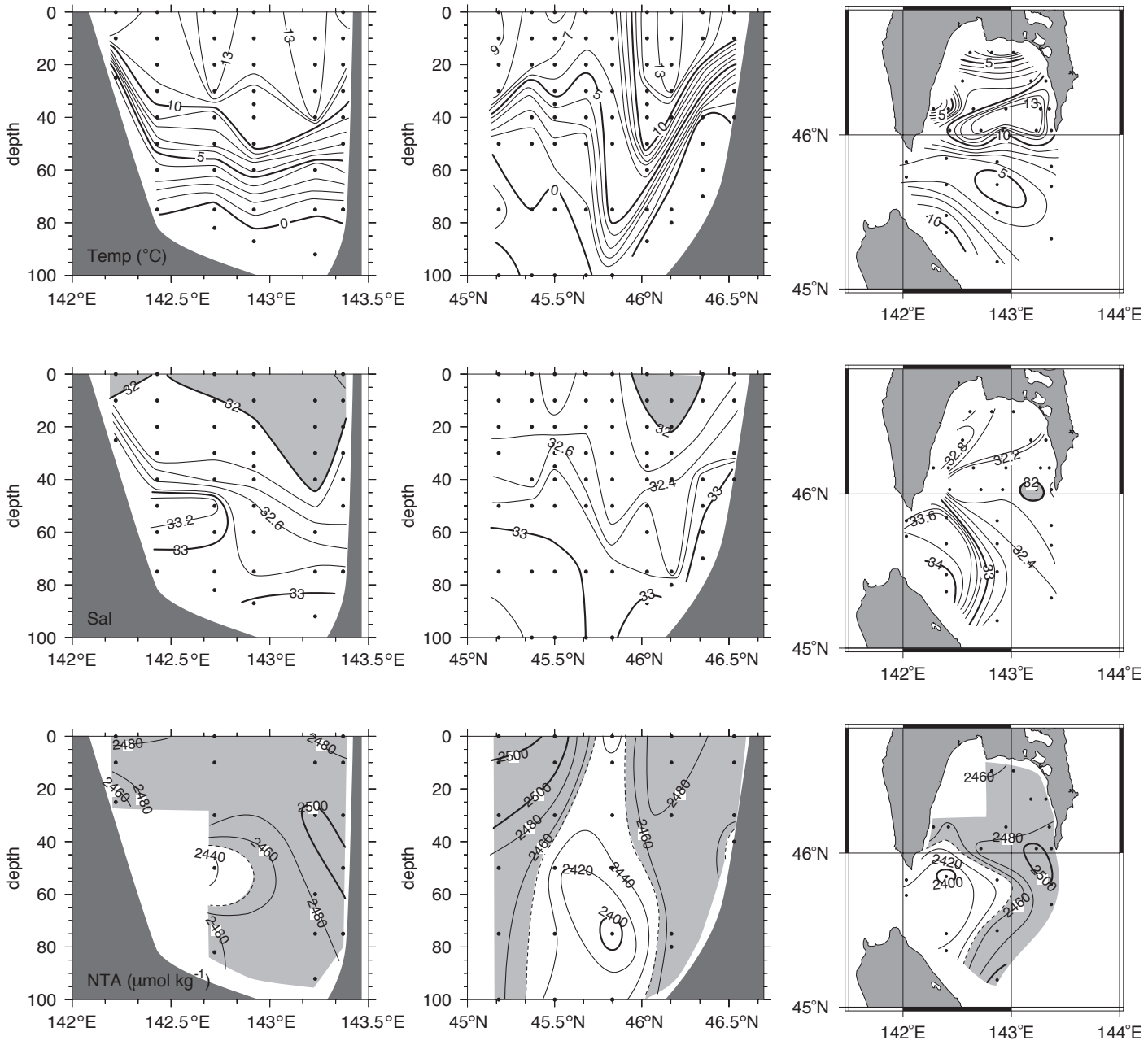

Figure 7 Oguma et al.

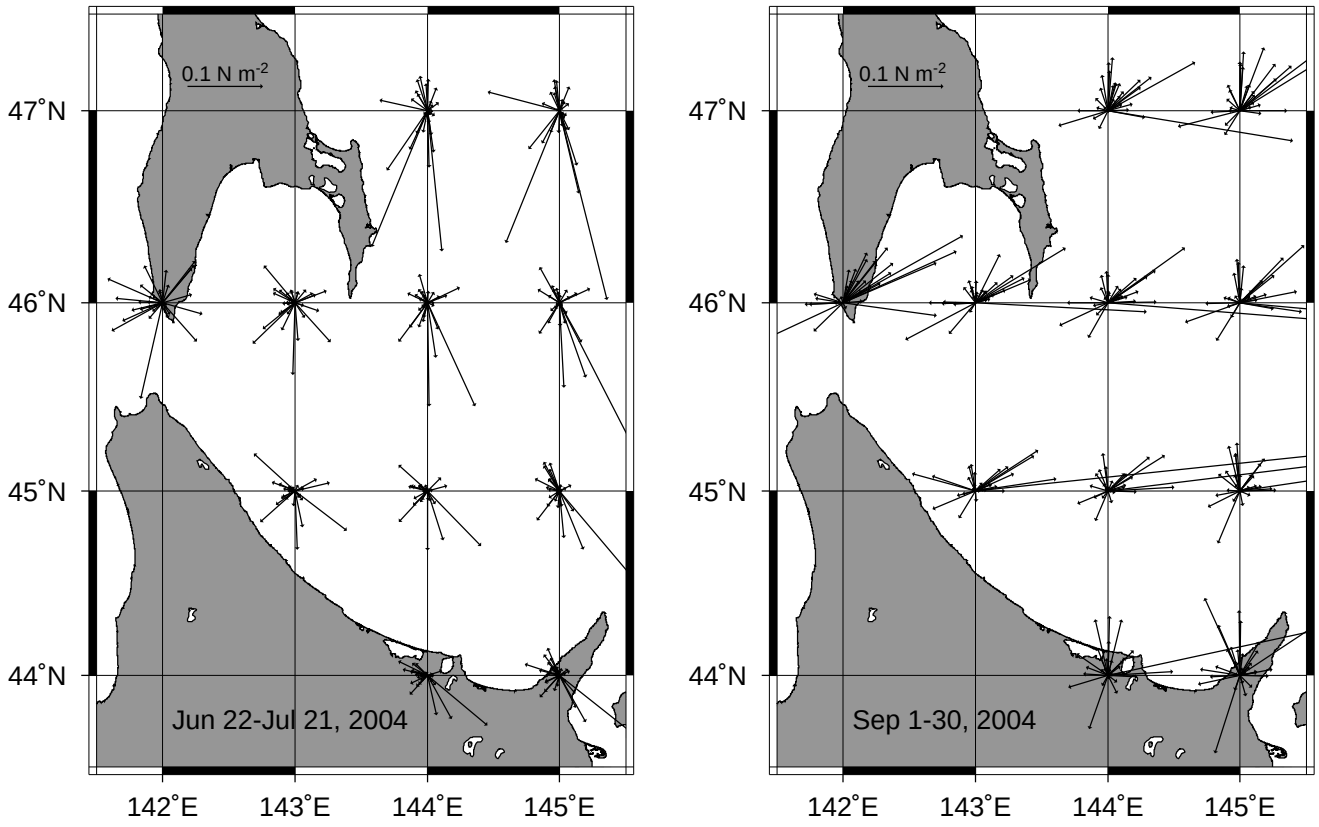

Figure 8

Oguma et al.